

---

## GENERALISED MODELS FOR TORSIONAL SPINE RECONNECTION

ALI KHALAF HUSSAIN AL-HACHAMI

*Dedicated to Professor S. S. Dragomir for his 60<sup>th</sup> birthday.*

*Received 5 July, 2019; accepted 16 December, 2019; published 31 January, 2020.*

DEPARTMENT OF MATHEMATICS, COLLEGE OF EDUCATION FOR PURE SCIENCES, WASIT UNIVERSITY,  
IRAQ.  
alhachamia@uowasit.edu.iq

**ABSTRACT.** Three-dimensional (3D) null points are available in wealth in the solar corona, and the equivalent is probably going to be valid in other astrophysical situations. On-going outcomes from sun oriented perceptions and from reproductions propose that reconnection at such 3D nulls may assume a significant job in the coronal dynamics. The properties of the torsional spine method of magnetic reconnection at 3D nulls are researched. Kinematic model are created, which incorporate the term  $\eta J$  that is spatially localised around the null, stretching out along the spine of the null. The null point is to research the impact of shifting the level of asymmetry of the null point magnetic field on the subsequent reconnection process where past examinations constantly considered a non-nonexclusive radially symmetric null. Specifically we analyse the rate of reconnection of magnetic flux at the spine of null point. Logical arrangements are determined for the enduring kinematic equation, and contrasted and the after effects of torsional spine reconnection models when the current is restricted in which the Maxwell conditions are illuminated. The geometry of the current layers inside which torsional spine reconnection happen is autonomous on the symmetry of the magnetic field. Torsional spine reconnection happens in a thin cylinder around the spine, with circular cross-segment when the fan eigenvalues are extraordinary. The short axis of the circle being along the solid field bearing. Just as it was discovered that the fundamental structure of the method of attractive reconnection considered is unaffected by changing the magnetic field symmetry, that is, the plasma flow is discovered rotational around the spine of null point. The spatiotemporal pinnacle current, and the pinnacle reconnection rate achieved, are found not to rely upon the level of asymmetry.

*Key words and phrases:* Magnetic fields, Magnetohydrodynamics (MHD), Sun: Corona.

*2010 Mathematics Subject Classification.* 00A71.

## 1. INTRODUCTION

There has been critical advancement lately towards understanding the properties of magnetic reconnection in three measurements (3D). Specifically, it is current valued that the exceptional current layers important for reconnection in astrophysical plasmas may shape at various distinctive trademark structures of the magnetic field. One such structure is a 3D magnetic null point. Such null point focuses have been shown to be available in wealth in the sun oriented crown (for example Longcope and Parnell 2009 [1]), and the equivalent is almost certain to be null in other astrophysical situations, for example, the crown of different stars and of accumulation plates. Ongoing outcomes from perceptions and re-enactments recommend that reconnection at these nulls may assume a significant job in the coronal elements (for example Luoni et al. 2007 [2]; Lynch et al. 2008[3]; Parlat et al. 2009[4]). Note likewise that the significance of reconnection at 3D nulls isn't limited to astrophysical plasmas, however assumes a job both in the Earth's magnetosphere (for example Xiao et al. 2006[6]) and some lab plasmas.

On-going examinations have uncovered various trademark methods of reconnection that may happen at such 3D nulls. These have as of late been ordered by Priest and Pontin (2009)[5] into 'torsional spine reconnection', 'torsional fan reconnection' and 'spine-fan reconnection'. Torsional spine and torsional fan reconnection happen when a balance magnetic null point field is bothered by a rotational irritation (the pivot being in a plane opposite to the spine). Spine-fan reconnection happens when a shear bother is connected that aggravates the areas of the spine and fan this prompts a confined current layer conforming to the null and flux transport over the fan separatrix surface. Near the null the magnetic field might be composed

$$(1.1) \quad \mathbf{B} = \nabla B \cdot \mathbf{x}$$

What's more, the eigenvalues and eigenvectors of the lattice  $\mathbf{B}$  decide the areas of the spine and aficionado of the null (see for example Parnell et al.1996[7]). Past investigations of the generation of current layers at 3D nulls because of rotational movements have considered just the situation where the foundation balance null point has a rotational symmetry, for example in which the two eigenvalues related with the fan are equivalent. Amid the subsequent advancement where torsional spine and torsional fan reconnection happens, the separate current layers, plasma flows, and so on, have shown azimuthal symmetry because of the azimuthally symmetric foundation magnetic fields and bothers. We have recently explored the impact of changing the symmetry of the foundation null point field on the spine-fan reconnection mode, and appeared while the topological properties of the reconnection are unaltered, the measurements and power of the present layer, and the reconnection rate, are unequivocally reliant on the level of asymmetry (Al-Hachami and Pontin 2010[8]), just as the relative edge between the shear driving and the solid/feeble field bearings (Galsgaard and Pontin 2011[9]). Pontin et al. (2011)[10] summed up existing models for torsional spine and torsional fan null point reconnection. For each situation by presenting another kinematic systematic answer for the comparing reconnection mode in which a restricted current layer is available at the null. In this paper we sum up model for spine reconnection. We start by sum up kinematic model, it was first appeared by Pontin et al. (2004)[11]. At that point we proceed to consider the impact of differing the symmetry of the foundation magnetic field, by changing the proportion of the fan eigenvalues of the null. In section 2 we survey past demonstrating of torsional spine reconnection. In section 3, we given a general strategy. In section 4 and 5, we depict a kinematic model for reconnection at a non-symmetric null point, contrasting our outcomes and those of Pontin et al. (2011)[10], at long last in section 6, we present our conclusions.

## 2. EXISTING MODELS FOR TORSIONAL SPINE RECONNECTION

Torsional spine reconnection includes the development of a current layer wherein the current vector is guided parallel to the spine line at the null. It was first appeared by Pontin et al. (2004)[11] that the relating reconnection appears as a rotational slippage of magnetic flux stringing the non-ideal region. (This is as opposed to the situation where the current vector is parallel to the fan, in which case magnetic flux is reconnected over the spine and fan (Pontin et al. 2005)[12]. The magnetic flux experiences this rotational slippage because of rotational streams in the perfect locale in which the rate of flux transport the azimuthal way is diverse for field lines entering the non-ideal region than it is for field lines leaving the non-ideal region. The first model of Pontin et al. (2004)[11] depends on the magnetic field

$$\mathbf{B} = B_0[r, jr/2, -2z]$$

in cylindrical polar coordinates. This results in a spatially uniform current parallel to the spine (z-axis). In order to obtain a 3D- localised non-ideal region (relevant in astrophysical plasmas which are approximately ideal almost everywhere), it was therefore necessary to impose a localised resistivity profile. In cylindrical polar coordinates. This outcomes in a spatially uniform current parallel to the spine (z-axis). So as to acquire a 3D- localised non-ideal region (applicable in astrophysical plasmas which are roughly perfect all over the place), it was in this manner important to force a restricted resistivity profile. In the accompanying section we explore the impact on our answer of differing the symmetry of the magnetic field. Pontin et al. (2011)[10] have contemplated the procedure of torsional spine and fan reconnection by setting up a kinematic, stationary MHD model with the non-ideal region being restricted, i.e., they have introduced arrangements of the MHD equations in which out of the blue incorporate a present layer that is spatially confined around the invalid, stretching out along the spine of the invalid. It is significant that extra kinematic arrangements with a spatially fluctuating current thickness have been exhibited by Wyper and Jain (2010)[13]. In their answers the current is spatially confined, yet as opposed to our new arrangements is centered far from the null point. Resistive MHD reenactments have shown that the type of the present layer is distinctive relying upon whether the rotational irritation principally exasperates the fan field lines or field lines around the spine. The annoyance carries on basically as an Alfvén wave, going along the magnetic field lines, which because of the hyperbolic structure of the field around the invalid prompts the irritation gathering either in the region of the spine or the fan. At the point when the fan field lines are exposed to a rotational unsettling influence, torsional spine reconnection happens in a rounded current structure that frames at the spine (Rickard and Titov 1996[14]; Pontin and Galsgaard 2007)[15]. Inside this cylinder, the magnetic field lines winding around the spine line. The span of the cylinder diminishes, and the current strengthens, until the winding of the field being driven by the annoyance is adjusted by rotational slippage encouraged by resistive diffusion. The reconnection rate, characterized in 3D as the maximal estimation of

$$(2.1) \quad \Psi = \int \mathbf{E} \cdot \mathbf{B}/|\mathbf{B}| dl$$

along any field line stringing the non-ideal region, at that point evaluates this rotational slippage. At the point when field lines in the region of the spine line are bothered, a present layer shapes on the fan surface prompting torsional fan reconnection (Rickard and Titov 1996[14]; Galsgaard et al. 2003[9]). Again field lines winding inside the current layer, whose extent escalates as the turning of the field is moved in an inexorably limited sheet over the fan surface. When the sheet turns out to be adequately thin resistive dissemination scatters the bend driving by and by to a rotational slippage of field lines.

### 3. GENERAL STRATEGY

We look to discover answers for the kinematic, steady state, resistive MHD equations in the region of a 3D magnetic null point. In this way, we comprehend

$$(3.1) \quad \mathbf{E} + \mathbf{v} \times \mathbf{B} = \eta \mathbf{J},$$

$$(3.2) \quad \nabla \times \mathbf{E} = 0,$$

$$(3.3) \quad \nabla \times \mathbf{B} = \mu_0 \mathbf{J},$$

$$(3.4) \quad \nabla \cdot \mathbf{B} = 0.$$

From Eq.3.2 we can express the electric field as  $\mathbf{E} = -\nabla\Phi$  where  $\Phi$  is a scalar potential. The part of Eq.3.1 parallel to  $\mathbf{B}$  can be joined with this and coordinated along the magnetic field lines to give

$$(3.5) \quad \Phi = - \int \eta \mathbf{J} \cdot \mathbf{B} ds + \Phi_0$$

This basic is tackled by utilizing the field line conditions  $(x, y, z)$  in communicated in term of the parameters  $s$  and some underlying position. The field line equations are gotten by illuminating

$$(3.6) \quad \frac{\partial \mathbf{X}(s)}{\partial s} = \mathbf{B}(\mathbf{X}(s)),$$

where  $\Phi_0$  is a steady of incorporation. These conditions are invertible so  $\Phi$  can be spoken to as a component of  $s$  and starting position to do the integral in Eq. 3.5 and after that moved once again into a component of  $x, y$  and  $z$  to locate the electric field from

$$(3.7) \quad \mathbf{E} = -\nabla\Phi$$

In this way for a given attractive arrangement we can locate the electric field due to non-ideal impacts i.e., those because of  $J \neq 0$ . At that point we can discover the plasma velocity opposite to the magnetic field,  $\mathbf{v}_\perp$ , by taking the vector result of Eq.3.1 with  $\mathbf{B}$  to get

$$(3.8) \quad \mathbf{v}_\perp = \frac{(\mathbf{E} - \eta \mathbf{J}) \times \mathbf{B}}{B^2}$$

### 4. KINEMATIC SOLUTION

#### 4.1. The model.

We initially consider the most immediate speculation of the model of Pontin et al. (2004)[11]. We take model with uniform current. In the event that a diffusion region is isolated, an adjustment in connectivity of field lines might be considered, by following field lines tied down in the perfect locale on opposite side of the dissemination area. A dispersion area is, when all is said in done, disengaged if  $\eta \mathbf{J}$  is localised in space. In down to earth cases in astronomy, this is probably going to be basically on the grounds that  $\mathbf{J}$  is confined be that as it may, what's more, now and then in light of the fact that as a result  $\eta$  is additionally limited. Al-Hachami and Pontin (2010)[8] have localised  $\eta$ , while Pontin et al. (2011)[10] have localised  $\mathbf{J}$ . Anyway the significant component in every one of these cases is that the item  $\eta \mathbf{J}$  is limited. Since we need a disconnected dispersion area,  $\eta \mathbf{J}$  ought to be limited in space. Subsequently, we force a spatially localisation of the resistivity together with a  $\mathbf{J}$  that isn't confined. The purpose behind doing this is to render the scientific conditions tractable. As in Al-Hachami and Pontin (2010)[8] and Pontin et al. (2011)[10], we look for an answer for the kinematic, steady, resistive MHD Equations in the area of an magnetic null point. That is, we understand Eqs.3.1-3.4. Though in

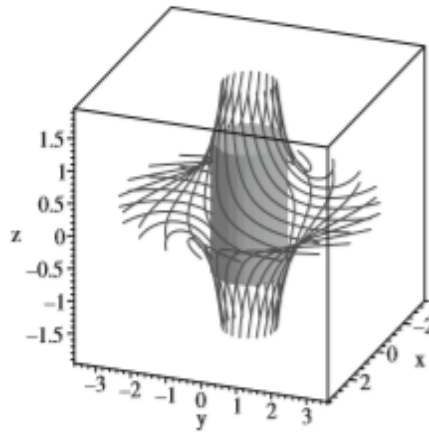


Figure 1: Schematic diagram of torsional spine reconnection at an isolated null. Black lines are magnetic field lines, The shaded surface shows is a current density isosurface.

Al-Hachami and Pontin (2010)[8] we analysed the kinematic conduct around an magnetic null point whose related current was parallel to the fan plane, here we are moving to explore the conduct of the attractive field in the region of an invalid point where the current ( $\mathbf{J}$ ) lies parallel to the spine. We pick the magnetic field to be

$$(4.1) \quad \mathbf{B} = \frac{B_0}{L_0} \left( \frac{2x}{p+1} - \frac{1}{2}j_0y, \frac{2py}{p+1} + \frac{1}{2}j_0x, -2z \right)$$

where  $p$  is a parameter (here we confine ourselves to the case  $p > 0$  without loss of simplification). The uncommon case  $p = 1$  relates to rotational symmetry about the invalid point which was contemplated by Pontin et al. (2004). The spine lies in the  $z$ -course, and the current is  $\mathbf{J} = (B_0/\mu_0)(0, 0, j_0)$  from Eq. (3.3), and is additionally coordinated along the  $z$ -axis, (i.e., we have an null with current guided parallel to the spine line see Figure 1). It is at first valuable to characterize  $Q = \frac{L}{2(p+1)}$ ,  $L = \sqrt{4p^2 - 8p + 4 - j_0^2p^2 - 2j_0^2p - j_0^2}$  such that, from the matrix  $\nabla\mathbf{B}$  (see Eq. 1.1), the eigenvalues are

$$\lambda_1 = \frac{B_0}{L_0} (1 + Q), \quad \lambda_2 = \frac{B_0}{L_0} (1 - Q), \quad \lambda_3 = -2\frac{B_0}{L_0}.$$

In line with Parnell et al. (1996) it is useful to defined a threshold current,

$$j_{threshold} = \sqrt{\frac{4(p-1)^2}{(p+1)^2}}.$$

Therefore,  $Q = \frac{1}{2}\sqrt{j_{threshold}^2 - j_0^2}$ , which leads to three different cases of eigenvalues we must consider.

- 1- If  $j_0^2 > j_{threshold}^2$ , we have complex conjugate eigenvalues ( $\det(\nabla\mathbf{B}) > 0$ ) see Figures 2a and 2b.
- 2- If  $j_0^2 < j_{threshold}^2$ , the eigenvalues become real ( $\det(\nabla\mathbf{B}) < 0$ ) see Figure 2c.
- 3- If  $j_0^2 = j_{threshold}^2$ , we have repeated eigenvalues see Figure 2d.

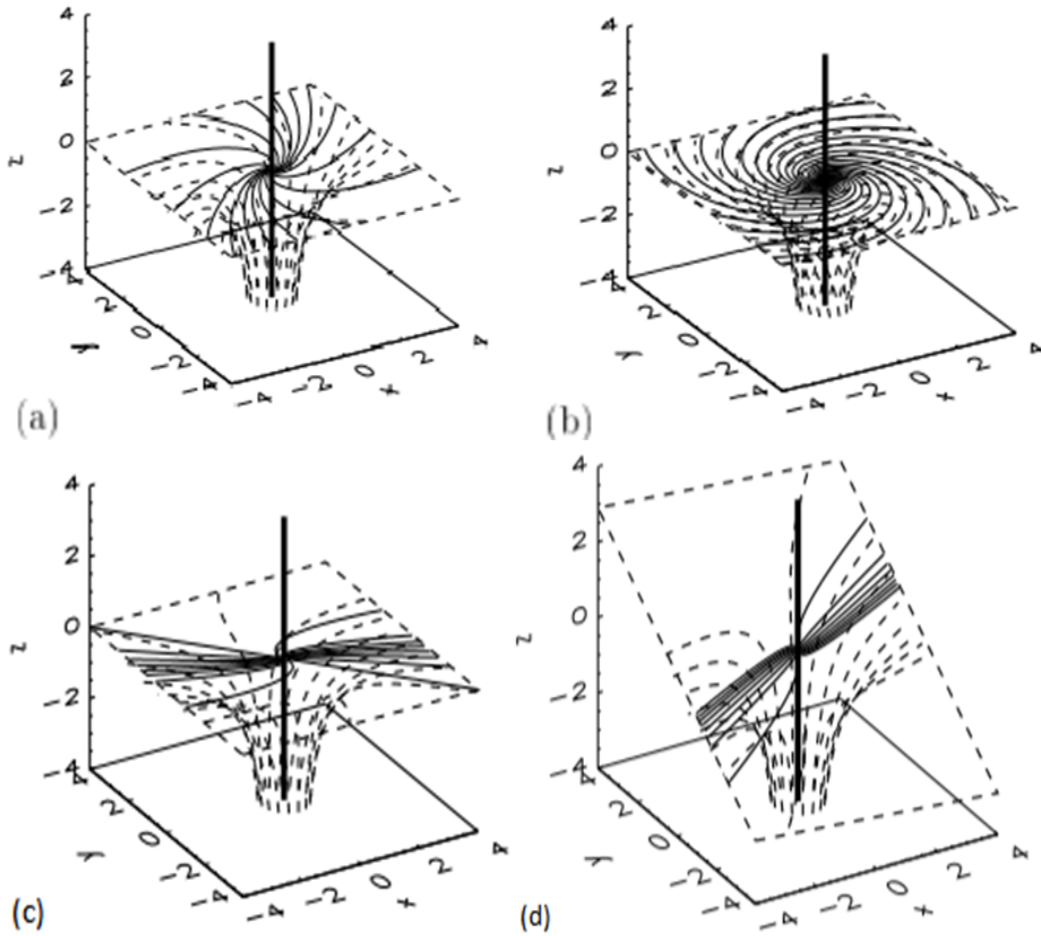


Figure 2: The magnetic field configurations of 3D non-potential fields (the fan plane  $xy$ -plane) with  $j_o = 1$  and different values of  $p$ : (a)  $p = 1$ , (b)  $p = 2$ , (c)  $p = 5$  and (d)  $p = 3$ , in the fan plane.

Notwithstanding these three cases we additionally have that the eigenvalues are constantly unpredictable when  $j_o > 2$  for all  $p$ . In the accompanying, we will talk about in detail every one of the above cases independently, in light of the fact that they require various treatments.

#### 4.2. $j_o^2 > j_{threshold}^2$

To begin with, let us consider the circumstance where the dimension of the part of current parallel to the spine is more prominent than that of the limit current. This suggests the two eigenvalues comparing to the eigenvectors that characterize the fan plane are mind boggling and field lines in this plane will be spirals (the fan and spine are perpendicular).

The eigenvalues of the null point for this situation are

$$\lambda_1 = \frac{B_0}{L_0} (1 + Q), \quad \lambda_2 = \frac{B_0}{L_0} (1 - Q), \quad \lambda_3 = -2 \frac{B_0}{L_0}.$$

where  $Q$  is imaginary, with corresponding eigenvectors

$$\mathbf{k}_1 = \begin{pmatrix} 1 \\ \frac{-2p+2-L}{j_o(p+1)} \\ 0 \end{pmatrix}, \quad \mathbf{k}_2 = \begin{pmatrix} 1 \\ \frac{-2p+2+L}{j_o(p+1)} \\ 0 \end{pmatrix}, \quad \mathbf{k}_3 = \begin{pmatrix} 0 \\ 0 \\ 1 \end{pmatrix}.$$

Since  $Q$  is fanciful, clearly the eigenvectors identifying with the eigenvalues will likewise be perplexing conjugates (the genuine and nonexistent piece of  $k_1$  and  $k_2$  will characterize the fan surface). For the attractive field characterized as in Eq. (4.1), shut structure articulations for the conditions of attractive field lines can be found, by utilizing Eq. (3.6) where the parameter  $s$  keeps running along field lines, to give

$$(4.2) \quad x = x_0 e^{\frac{B_0}{L_0} s(1+Q)} \cos Qs + \frac{(y_0 j_o p + y_0 j_o + 2x_0 p - 2x_0) e^{\frac{B_0}{L_0} s(1-Q)}}{L},$$

$$(4.3) \quad y = \frac{e^{\frac{B_0}{L_0} s(1+Q)} (-L \sin Qs + \cos Qs(2p - 2))}{j_o(p + 1)} + \frac{1}{L j_o(p + 1)}$$

$$(y_0 j_o(p + 1) + 2x_0(p - 1))(\sin Qs(2p - 2) + \cos QsL) e^{\frac{B_0}{L_0} s(1-Q)},$$

$$(4.4) \quad z = z_0 e^{-2\frac{B_0}{L_0} s},$$

with the inverse mapping  $\mathbf{X}_0(\mathbf{x}_0, s)$  given by

$$(4.5) \quad x_0 = e^{-\frac{B_0}{L_0} s(1+Q)} \left( \frac{\sin(Qs)(y_j o p + y_j o - 2x + 2px) + Lx \cos(Qs)}{L} \right),$$

$$(4.6) \quad y_0 = e^{-\frac{B_0}{L_0} s(1-Q)} \left( \frac{\cos(Qs)(-y_j o p - y_j o + 2x - 2px) + Lx \sin(Qs)}{L} \right),$$

$$(4.7) \quad z_0 = z e^{2\frac{B_0}{L_0} s}.$$

We currently continue to explain equations (3.1-3.4) by utilizing the general strategy portrayed in section 3. As we have notice previously, so as to have a restricted non-ideal term  $\eta \mathbf{J}$  we need to confine the resistivity as we referenced previously, since  $\mathbf{J}$  is consistent. Note that in the event that we endorse ? we can generally ascertain  $\Phi$  from the part of Eq.(3.1) parallel to  $\mathbf{B}$ ,  $-(\nabla \Phi)_{\parallel} = \eta \mathbf{J}_{\parallel}$  by utilizing Eq. (3.5). Substituting equations (4.2-4.4) into the integrand of Eq. (3.5), we can play out this incorporation to acquire  $\Phi(\mathbf{X}_0, s)$ . When this is done, we use Eqs.(4.5-4.7) to take out,  $x_0$  and  $y_0$  to get  $\Phi(\mathbf{X})$ , treating  $z_0$  as a consistent. By and large we characterize  $\eta$  in a piecewise way to have the option to tackle for  $s$  on the limit of dissemination area (this infers additionally that all field lines must cut every one of the top surface and side surface of the round and hollow non-perfect district once and just once). In any case, for this situation we were unfit to locate any such surfaces to bound the dispersion locale which fulfill these conditions. We in this manner take  $\eta$  to be of the structure

$$(4.8) \quad \eta = \eta_0 e^{\left(-\frac{R^2}{a^2} - \frac{z^2}{b^2}\right)}$$

where  $R = \sqrt{x^2 + py^2}$  and  $\eta_0, a$  and  $b \in \mathbb{R}^+$ . This has the impact of misshaping the current into a barrel with curved cross-area, with major and minor tomahawks along the  $x$ -and  $y$ - axes, stretching out to  $x = a, y = a/p$ . We utilize Maple's inbuilt *newtoncotes6* method to understand Eq. 3.5 where  $101^3$  gridpoints are utilized over the space  $-2 \leq x, y \leq 2, 0 \leq z \leq 2$ . The careful profile of  $\eta$ , given by Eq. (4.8), is picked with the end goal that the component of the dispersion district is constrained by the parameters  $a$  and  $b$ , where  $a$  controls the span and  $b$  the tallness. The electric field  $\mathbf{E}$  can thusly be found by utilizing a limited contrast (we utilize a five point limited distinction to process the numerical subordinate of  $\Phi$  to figure the electric field  $\mathbf{E}$ ) strategy and the plasma velocity opposite to the field,  $\mathbf{v}_{\perp}$  by utilizing Eq. (3.8).

4.3.  $j_o^2 < j_{threshold}^2$ .

For the situation where the size of the part of current parallel to the spine is not as much as that of the edge current, each of the three eigenvalues are genuine and we have comparing eigenvectors

$$\mathbf{k}_1 = \begin{pmatrix} 1 \\ \frac{-2p+2-L}{j_o(p+1)} \\ 0 \end{pmatrix}, \quad \mathbf{k}_2 = \begin{pmatrix} 1 \\ \frac{-2p+2+L}{j_o(p+1)} \\ 0 \end{pmatrix}, \quad \mathbf{k}_3 = \begin{pmatrix} 0 \\ 0 \\ 1 \end{pmatrix},$$

so the fan and spine are perpendicular and the field lines in the plane of the fan become parallel to the line,

$$y = \frac{(-2p + 2 + L)}{j_o(p + 1)}x,$$

close to the null, and

$$y = \frac{(-2p + 2 - L)}{j_o(p + 1)}x$$

when far from the null. From Equation(3.6) the field line equations are:

$$(4.9) \quad x = \frac{x_0(L - 2p + 2) - y_0(j_o p + j_o)}{2L} e^{\frac{B_0}{L_0} s(1+Q)} + \frac{y_0(j_o p + j_o) + x_0(2p - 2 + L)}{2L} e^{\frac{B_0}{L_0} s(1-Q)}$$

$$(4.10) \quad y = -\frac{(2p - 2 + L)(x_0(L - 2p + 2) - y_0(j_o p + j_o))}{2j_o(p + 1)L} e^{\frac{B_0}{L_0} s(1+Q)} + \frac{(-2p + 2 + L)(y_0(j_o p + j_o) + x_0(2p - 2 + L))}{2j_o(p + 1)L} e^{\frac{B_0}{L_0} s(1-Q)}$$

$$(4.11) \quad z = z_0 e^{-2\frac{B_0}{L_0} s}$$

with the inverse mapping  $\mathbf{X}_0(\mathbf{x}_0, s)$ , given by

$$(4.12) \quad x_0 = \frac{x(-2p + 2 + L) - y(j_o p + j_o)}{2L} e^{-(1+Q)\frac{B_0}{L_0} s} + \frac{x(-2 + L + 2p) + y(j_o p + j_o)}{2L} e^{-(1+Q)\frac{B_0}{L_0} s}$$

$$(4.13) \quad y_0 = \frac{x(4 + 4p^2 - L^2 - 8p) + y(2p^2 - 2 + j_o L + j_o L p)}{2j_o L(p + 1)} e^{-(1+Q)\frac{B_0}{L_0} s} - \frac{x(4p^2 - 8p + 4L^2) + y(2p^2 j_o - 2j_o - j_o L - j_o L p)}{2j_o L(p + 1)} e^{-(1+Q)\frac{B_0}{L_0} s}$$

$$(4.14) \quad z_0 = z e^{2\frac{B_0}{L_0} s}.$$

Note that here all the terms are real, since we have real eigenvalues. Now it is possible, by the method that was already explained in 3 of this section, to find  $\mathbf{E}$  and  $\mathbf{v}_\perp$

4.4.  $j_o^2 = j_{threshold}^2$ .

In the case where the current parallel to spine and threshold current are equal, we find that the two of the eigenvalues are repeated so have only one associated eigenvector, such that

$$\lambda_{1,2} = \frac{B_0}{L_0}, \quad \lambda_3 = -\frac{2B_0}{L_0},$$

and the eigenvectors are, respectively,

$$\mathbf{k}_{1,2} = \begin{pmatrix} -1 \\ 1 \\ 0 \end{pmatrix}, \quad \mathbf{k}_3 = \begin{pmatrix} 0 \\ 0 \\ 1 \end{pmatrix}.$$

So the field lines lying in the plane of the fan directed away from the null and form what looks like a spiral null (critical spiral) (Parnell et al. 1996). The field lines in the plane of the fan become parallel to the line

$$y = -x,$$

both as they approach the null and as they approach infinity. From Eq. 3.6 we can find the field line equations, which are

$$(4.15) \quad x = x_0 e^{\frac{B_0}{L_0} s(1+Q)} - \frac{p-1}{p+1} (x_0 + y_0) e^{\frac{B_0}{L_0} s(1-Q)},$$

$$(4.16) \quad y = -x_0 e^{\frac{B_0}{L_0} s(1-Q)} + \frac{p-1}{p+1} (x_0 + y_0) s e^{\frac{B_0}{L_0} s(1-Q)},$$

$$(4.17) \quad z = z_0 e^{-2\frac{B_0}{L_0} s}.$$

The inverse of Eqs (4.15-4.17) are:

$$(4.18) \quad x_0 = e^{-\frac{B_0}{L_0} s(1+Q)} \left( \frac{pys + xp + xps + x + sy - xs}{p+1} \right),$$

$$(4.19) \quad y_0 = e^{-\frac{B_0}{L_0} s(1-Q)} \left( -\frac{pys - yp + xps - y - sy - xs}{p+1} \right),$$

$$(4.20) \quad z_0 = z e^{2\frac{B_0}{L_0} s}.$$

The method used to calculate  $\mathbf{E}, \mathbf{v}_\perp$  is the same as before.

## 5. KINEMATIC SOLUTION-ANALYSES

### 5.1. The plasma flow.

We analyze in this segment the idea of the arrangement in the three unique cases. We might now want to research how the properties of the arrangement differ when the rotational symmetry of the above framework is broken. We may break the symmetry in the potential segment characterizing the attractive invalid. Hence as  $p$  fluctuates the attractive field along the spine bearing is fixed while the proportion between the fan eigenvalues (related with the eigenvectors along the  $\hat{x}$  and  $\hat{y}$  headings) shifts. To coordinate Eq. (3.5) we set  $s = 0$  on  $z = \pm z_0$  ( $z_0 = 2b$ ), in this manner  $\Phi$  is consistent for  $z > b$ . We set  $B_0 = L_0 = \eta_0 = j_o = 1, a = 1, b = 2$ , and understand Eq. 3.8 with the arrangement start symmetry about  $z$ . We limit our thoughtfulness regarding the range  $p > 1$ , which basically chooses the  $\hat{y}$  course as the solid field bearing in

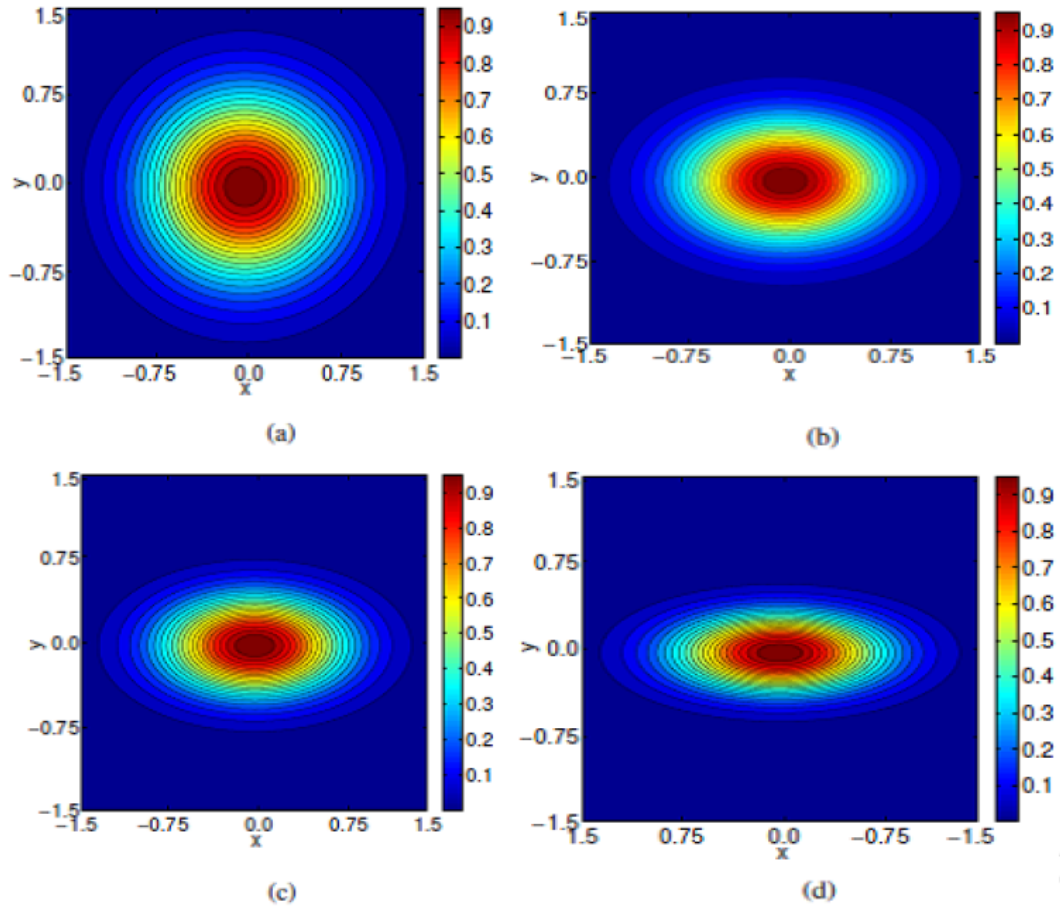


Figure 3: Diffusion region ( $\eta\mathbf{J}$ ) for the torsional spine kinematic solution. In the plane  $z = 0.01$ , with different  $p$  (a) at  $p = 1$ , (b)  $p = 2$ , (c)  $p = 3$ , (d)  $p = 5$ , for the parameters  $B_0=1$ ,  $a = 1$ ,  $b = 2$ ,  $\eta_0=1$ ,  $j_o = 1$ .

the fan. The consequence of the above investigation is available in Figs. 3-4. We find when  $p$  expanded, the dispersion area ends up topsy-turvy in the  $xy$ -plane, with rule current part  $j_z$  (see Fig.3).

The plasma velocity for  $0 < z < b$  is rotational around the spine inside the dispersion district which has a curved cross-segment when  $p \neq 1$ . Again there is no stream crosswise over either the spine or the fan. So as to demonstrate the outcomes all the more obviously, we will utilize the opportunity of discretionary stream parallel to  $\mathbf{B}$  in the model we can for illustrative purposes include a segment  $v_{||}$  with the end goal that  $v_z = 0$ .

$$(5.1) \quad \mathbf{v} = \mathbf{v}_{\perp} - \frac{(\mathbf{v}_{\perp})_z}{B_z} \mathbf{B}.$$

This is helpful to indicate plots of the vector field in the plane of steady  $z$ , without smothering any data, since now the speed has just  $x$  and  $y$  segments (see Figure 4). It is obvious from Figure 4 demonstrates that the diffusion region  $\eta\mathbf{J}$  reaches out in the  $x$ -direction when  $p > 1$ , i.e rotational plasma streams along elliptical ways are as yet present around the spine axis of null, like those found by Pontin et al. (2011)[10], one distinction between these models is that the two indications of rotational flow are seen amid a specific period in the our model. We can utilize a similar strategy with respect to  $z > 0$  to discover an answer for  $z < 0$  by incorporating from  $z = -b$ .

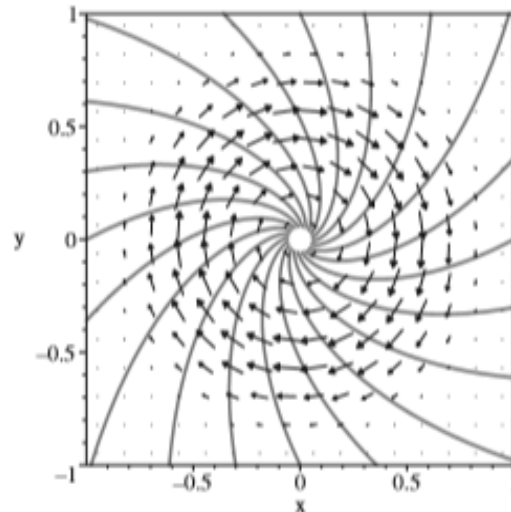


Figure 4: Vectors of the plasma flow  $v$ , along with a projection of the magnetic field lines in the plane  $z = 0.4$ , for the parameters  $B_0=1$ ,  $a = 1$ ,  $b = 2$ ,  $\eta_0=1$ ,  $j_o = 1$ .

### 5.2. Reconnection rate.

The rate of reconnected transition, when all is said in done, is given by the maximal indispensable of the parallel electric field  $E_{||}$  along any field line stringing a spatially limited dispersion area  $D$ . In two dimensional models the reconnection line is the augmentation of the hyperbolic null point along the invariant heading. We will consider only the motion reconnection in the half-spaces  $z > 0$ . At the point when the current is parallel to the spine, at that point there are counter-rotational stream, fixated on the spine, as here, this evaluates a rotational slippage of flux (Pontin et al. 2004)[11] see Figure 5.

Accordingly from Eq. (2.1) the reconnection rate,  $F$ , is the vital over the parallel electric field along the spine axis, is given by

$$\Psi = \int_0^\infty E_z dz = \Phi(x = y = 0, z = \infty) - \Phi(x = y = 0, z = 0) = \frac{\sqrt{\pi}}{2}bjB_0\eta_0.$$

In this work, the reconnection appears as a rotational slippage of magnetic flux stringing the non-ideal region, we found the reconnection rate is totally extraordinary to the circumstance consider in the past work (Pontin et al. 2005), where  $\mathbf{J}$  is parallel to the fan plane of null point, and there is an impact of the dissemination area and parameters an  $a$  and  $p$  on the rate of reconnection. Here the aftereffect of reconnection rate is needy of the parameter  $b$ .

### 6. CONCLUSION

Give us now a chance to examine our significant outcomes. Right off the bat, we have looked into definite systematic arrangements (kinematic solution) portraying attractive reconnection in three measurements where the magnetic null point was characterized by

$$\mathbf{B} = \frac{B_0}{L_0} \left( \frac{2x}{p+1} - \frac{1}{2}j_oy, \frac{2py}{p+1} + \frac{1}{2}j_ox, -2z \right)$$

. This magnetic field has current adjusted to the spine line of the invalid point, and Pontin et al. (2004) considered this circumstance in the non-nonexclusive symmetric case  $p = 1$

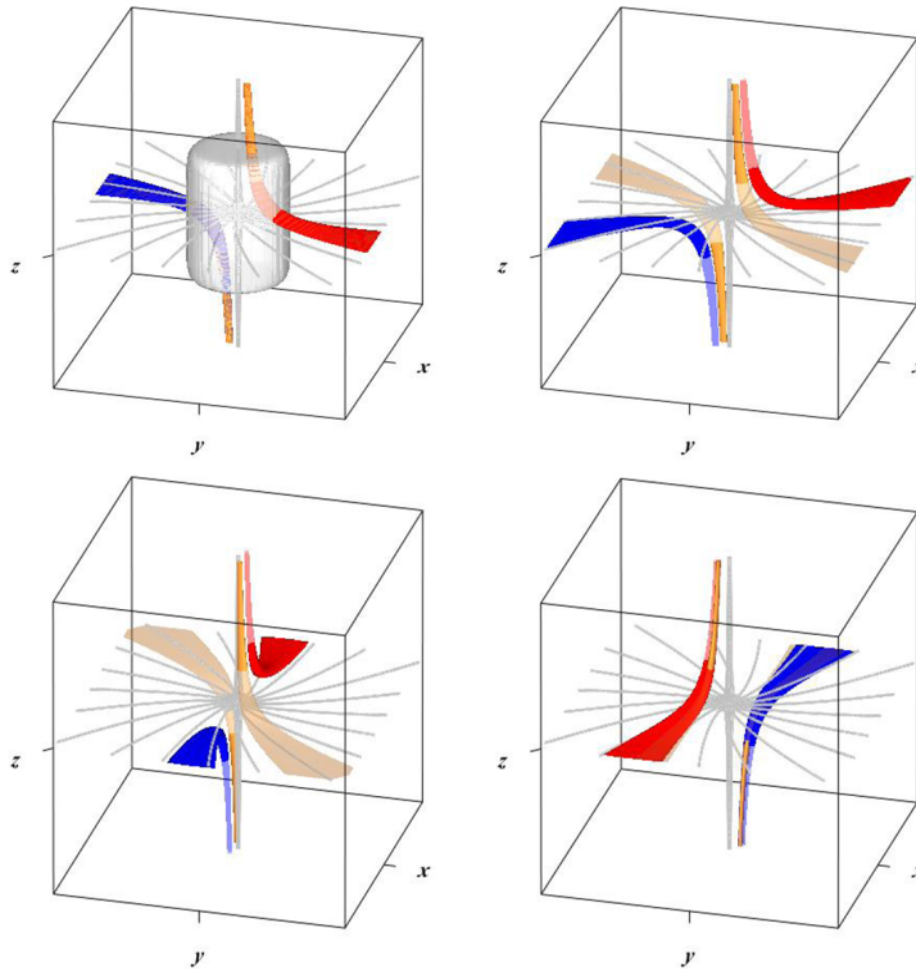


Figure 5: Reconnection of two representative flux tubes in the magnetic field Eq.4.1 at  $p = 1$ , corresponding to current directed parallel to the spine with ( $j_o = 1$ ). A localised diffusion region is present around the null point, shown by the shaded surface in the first time.

(complex eigenvalues). In this work, we think about  $p$  as a parameter. Our new model shows a similar structure of plasma flow as past torsional spine reconnection models i.e., just a single indication of rotational stream because of the way that we have a uniform current. Likewise we found that the reconnection rate is autonomous of  $p$ , this is totally extraordinary with Pontin et al. (2011)[8] models where they found that the geometry of the present layers inside which torsional spine reconnection happen is unequivocally reliant on the symmetry of the magnetic field characterizing the null point. 3D null points have been shown to be available in plentitude in the sun based crown, and the equivalent is probably going to be valid in other astrophysical conditions. Ongoing outcomes from sun powered perceptions and from reproductions propose that reconnection at such 3D nulls may assume a significant job in the coronal elements. The fan separatrix surfaces of these 3D nulls partition the coronal attractive field into particular topological areas, for example particular areas of attractive network between the photospheric transition fixations. The torsional spine reconnection mode don't act to exchange attractive transition between these topological areas, yet rather grant a rotational slippage inside the spaces of the attractive motion lying near the nulls and subsequently the area limits. These null point reconnection modes are accordingly probably not going to be engaged with lively occasions that include a huge scale rebuilding of the magnetic flux between topological areas as the coronal

field looks for a lower vitality state (for example during solar flares). Or maybe, they are a component to disseminate vitality and diminish pressure related with the dynamic annoyance of the coronal field by the tempestuous limit driving from the photosphere.

Torsional spine reconnection still happens in a limited cylinder around the spine, yet with circular cross-area when the fan eigenvalues are extraordinary. The unpredictability of the oval increments as the level of asymmetry increments, with the short axis of the circle being along the solid field course. The kinematic arrangements recommend that the current, and the reconnection rate achieved, don't rely upon the level of asymmetry.

## REFERENCES

- [1] D. W. LONGCOPE, and C. E. PARNELL, The number of magnetic null points in quiet sun corona, *Solar Phys.*, **254** (2009), pp. 51–75.
- [2] M. L. LUONI, H. H. MANDRINI, G. D. CRISTIANI, and DEMOULIN, The magnetic field topology associated to two M flares, *Space Res.*, **1382** (2007), pp. 39–53.
- [3] G. J. LYNCH, S. K. ANTIOCHOS, C. R. DEVORE, J. G. LUHMANN, and T. H. ZURBUCHEN, Topological evaluation of fast magnetic breakout CME in the three dimensions, *Astrophys. J.*, **683** (2008), pp. 1192–1206.
- [4] E. PARIAT, S. K. ANTIOCHOS, and C. R. DEVORE, 3-D modeling of quasi-homologous solar jet, *Astrophys. J.*, **691** (2009), pp. 61–75.
- [5] E. R. PRIEST, and D. I. PONTIN, 2009, 3d null point reconnection regimes, *Phys. Plasmas*, **16** (2009), pp. 101–122.
- [6] C. J. XIAO, X. G. WANG, Z. Y. PU, et al., In situ evidence for the structure of the magnetic null in a 3d reconnection event in the earth's magnetotail, *Nature Physics*, **2** (2006), pp. 4781–483.
- [7] C. E. PARNELL, J. M. SMITH, T. NEUKIRCH, and E. R. PRIEST, The structure of three-dimensional magnetic neutral points, *Phys. Plasmas*, **3** (1996), pp. 759–770.
- [8] A. K. AL-HACHAMI, and D. I. PONTIN, Magnetic reconnection at 3d null points: effect of magnetic field asymmetry, *Astronomy and Astrophysics*, **512** (2010), A84.
- [9] K. GALSGAARD, and D. I. PONTIN, Steady state reconnection at a single 3D magnetic null point, *Phys. Plasmas*, **529** (2011), 20.
- [10] D. I. PONTIN, A. K. AL-HACHAMI, and K. GALSGAARD, Generalised models for torsional spine and fan magnetic reconnection, *Astronomy and Astrophysics*, **533** (2011), A78.
- [11] D. I. PONTIN, G. HORNIG, and E. R. PRIEST, Kinematic reconnection at a magnetic null point: Spine-aligned current, *Geophys. Astrophys. Fluid Dynamics*, **98** (2004), pp. 407–428.
- [12] D. I. PONTIN, and I. J. D. CRAIG, Current singularities at finitely compressible three-dimensional magnetic null points, *Phys. Plasmas*, **12** (2005), 77.
- [13] P. WYPER, and JAIN, Torsional magnetic reconnection at three dimensional null points: A phenomenological study, *Phys. Plasmas*, **9** (2010), 17.
- [14] G. J. RICKARD, and V. S. TITOV, Current accumulation at a three dimensional magnetic null, *Astrophys. J.*, **472** (1996), pp. 840–852.
- [15] G. J. RICKARD, and V. S. TITOV, Current accumulation at a three dimensional magnetic null, *J. Geophys. Res.*, **112** (2007), A03103.
- [16] K. GALSGAARD, E. R. PRIEST, and V. S. TITOV, Numerical experiments on wave propagation toward a 3d null point due to rotational motions, *J. Geophys. Res.*, **108** (2003), pp. 1042–1051.